



# Niacin bound chromium treatment induces myocardial Glut-4 translocation and caveolar interaction via Akt, AMPK and eNOS phosphorylation in streptozotocin induced diabetic rats after ischemia-reperfusion injury

Suresh Varma Penumathsa<sup>a,1</sup>, Mahesh Thirunavukkarasu<sup>a,1</sup>, Samson Mathews Samuel<sup>a</sup>, Lijun Zhan<sup>a</sup>, Gautam Maulik<sup>b</sup>, Manashi Bagchi<sup>c</sup>, Debasis Bagchi<sup>c</sup>, Nilanjana Maulik<sup>a,\*</sup>

<sup>a</sup> Molecular Cardiology and Angiogenesis Laboratory, Department of Surgery, University of Connecticut Health Center, 263 Farmington Avenue, Farmington, CT 06030-1110, USA

<sup>b</sup> Department of Thoracic Surgery, Harvard Medical School, Boston, MA, USA

<sup>c</sup> InterHealth Research Center, Benicia, CA, USA

## ARTICLE INFO

### Article history:

Received 23 June 2008

Received in revised form 18 October 2008

Accepted 20 October 2008

Available online 5 November 2008

### Keywords:

Chromium

Diabetes

eNOS

Heart

Glut-4

Ischemia reperfusion

## ABSTRACT

Diabetes, one of the major risk factors of metabolic syndrome culminates in the development of Ischemic Heart Disease (IHD). Refined diets that lack micronutrients, mainly trivalent chromium ( $\text{Cr}^{3+}$ ) have been identified as the contributor in the rising incidence of diabetes. We investigated the effect of niacin-bound chromium (NBC) during ischemia/reperfusion (IR) injury in streptozotocin induced diabetic rats. Rats were randomized into: Control (Con); Diabetic (Dia) and Diabetic rats fed with NBC (Dia+NBC). After 30 days of treatment, the isolated hearts were subjected to 30 min of global ischemia followed by 2 h of reperfusion. NBC treatment demonstrated significant increase in left ventricular functions and significant reduction in infarct size and cardiomyocyte apoptosis in Dia+NBC compared with Dia. Increased Glut-4 translocation to the lipid raft fractions was also observed in Dia+NBC compared to Dia. Reduced Cav-1 and increased Cav-3 expression along with phosphorylation of Akt, eNOS and AMPK might have resulted in increased Glut-4 translocation in Dia+NBC. Our results indicate that the cardioprotective effect of NBC is mediated by increased activation of AMPK, Akt and eNOS resulting in increased translocation of Glut-4 to the caveolar raft fractions thereby alleviating the effects of IR injury in the diabetic myocardium.

© 2008 Elsevier B.V. All rights reserved.

## 1. Introduction

The incidence of diabetes is associated with various risk factors such as obesity, increasing age, physical inactivity, autoimmune diseases, pancreatitis, viral infections etc. In addition to these risk factors, certain nutritional deficiencies have also been associated with a higher incidence of diabetes [1]. Chromium deficiency has been associated with elevated blood glucose levels and diabetes [1]. Chromium (Cr) is an essential micronutrient that is required for normal carbohydrate and lipid metabolism [1]. Highly refined diets that may be deficient in micronutrients, mainly trivalent chromium ( $\text{Cr}^{3+}$ ) have been identified as the dominant factor in the rising incidence of diabetes. However, the exact mechanism by which  $\text{Cr}^{3+}$  plays an important role in the regulation of glucose metabolism remains elusive. Furthermore,  $\text{Cr}^{3+}$  seems to have a role in increasing the tyrosine kinase activity of the insulin receptor [2–5]. Different forms of trivalent chromium such as chromium chloride ( $\text{CrCl}_3$ ) and chromium picolinate have been studied with respect to Type II

diabetes or Non-Insulin Dependent Diabetes Mellitus (NIDDM) but not Type I diabetes or Insulin Dependent Diabetes Mellitus (IDDM) [5–7]. In addition, Trueblood et al. has shown that niacin protects the isolated heart from ischemia-reperfusion injury [8] by lowering the cytosolic redox state and increasing the lactate efflux rate, consistent with redox regulation of glycolysis.

The regulation of glucose uptake and its utilization is critical for the maintenance of glucose homeostasis. Insulin plays a significant role in controlling the rates of glucose uptake, glycogen synthesis and glycolysis in the cardiac muscle. It is well established that glucose uptake is regulated by glucose transporter (Glut-4) in the plasma membrane [9]. It has been reported that increased glucose uptake in ischemic cardiomyocytes is achieved primarily by the translocation of Glut-4 from its intracellular compartments to the caveolae of the plasma membrane [10–12]. The caveolae are small flask shaped invaginations (50–100 nm in diameter) which act as the membrane organizing centers and signaling microdomains of the plasma membrane in almost all cell types, predominantly in the endothelial cells, myocytes and the adipocytes [10,13–16]. The structural proteins (the caveolins, Cav-1, Cav-2, Cav-3), sphingolipids and cholesterol are the main components of the caveolae [13]. These structural proteins serve as scaffolds and regulators of many proteins [16]. The M-

\* Corresponding author. Tel.: +1 860 679 2857; fax: +1 860 679 2825.

E-mail address: [nmaulik@neuron.uchc.edu](mailto:nmaulik@neuron.uchc.edu) (N. Maulik).

<sup>1</sup> Both authors contributed equally.

caveolin (Cav-3) is expressed in the muscle while Cav-1 is expressed in endothelial cells [17,18]. Studies in Cav-3<sup>-/-</sup> mice have shown that the absence of caveolin-3 leads to insulin resistance and increased adiposity [19]. It has also been reported that caveolin-1 acts like a physiological inhibitor of eNOS and that Cav-1 expression is upregulated in diabetic NOD mice [20]. eNOS derived NO is key enhancer of vascular functions, vessel relaxation and survival of vascular endothelial cells. The phosphorylation of eNOS at Ser1177 is said to render more activity to the protein. It is demonstrated that Akt/PKB phosphorylates eNOS at Ser1177 [21]. However, dominant negative Akt mutants were unable to block the phosphorylation of eNOS thereby showing an alternative mechanism for the activation of eNOS [22]. In this context, AMP-activated protein kinase (AMPK) has been shown to be involved in eNOS activation by enhancing its phosphorylation [23,24]. AMPK, a serine threonine kinase is known to be the metabolic master switch that senses and regulates the cellular energy status in various cell types [24,25]. Furthermore, phosphorylation of AMPK (pAMPK) and thus its activation has been associated with increased Glut-4 translocation and therefore increased glucose uptake in the myocardium [26,27]. We have demonstrated earlier that redox regulation of ischemic preconditioning is by differential activation of caveolin-1 and caveolin-3 and their association with eNOS and Glut-4 in which AMPK is also involved [10].

In conjunction with the previous reports including ours, in this study we investigated the effect of niacin-bound chromium (NBC) (commercially known as ChromeMate<sup>®</sup>) against ischemia/reperfusion (IR) injury in streptozotocin induced diabetic rats. We also investigated the effect of NBC on the activation of Akt, AMPK and eNOS and its role in the regulation of Glut-4 translocation to the membrane by modulating the levels of Cav-1 and Cav-3, in the diabetic myocardium.

## 2. Materials and methods

### 2.1. Animals

This study was performed in accordance with the principles of laboratory animal care formulated by the National Society for Medical Research and the Guide for the Care and Use of Laboratory Animals prepared by the National Academy of Sciences and published by the National Institutes of Health (Publication No. 85-23, revised 1985). The experimental protocol was examined and approved by the Institutional Animal Care Committee of the Connecticut Health Center (Farmington, CT). All animals used in the study received humane care and treatment. Male Sprague Dawley rats (275–300 g) were used for the study. Experimental diabetes was induced in the animals by a one time intraperitoneal administration of streptozotocin (STZ; Sigma, St Louis, MO) at a dosage of 65 mg kg<sup>-1</sup> in saline. Control rats received an equal volume of normal saline (i.p.). Blood was drawn from the rats by tail snip, five days after STZ injection, and blood glucose levels were measured using glucose monitoring system (Thera Sense, Inc. Alameda, CA, USA). Rats with blood glucose concentrations  $\geq 300$  mg/dl were considered to be diabetic.

### 2.2. Experimental protocol

Rats were randomly divided into 3 groups ( $n=24$  in each group): 1) Non-diabetic control rats (Con); 2) Diabetic rats (Dia); 3) Diabetic rats fed with diet containing Niacin-Bound Chromium (NBC) (Dia+NBC). Niacin bound chromium III complex commercially known as ChromeMate<sup>®</sup> was obtained from Inter Health Nutraceuticals, Benecia, CA, USA. The chromium dosage for an adult weighing 70 kg is 4 mg. For a rat weighing 250–275 g it is 0.0145 mg and considering a 5 fold faster metabolism in the case of rat [28] the daily chromium dose will be 5 times more i.e. 0.0727 mg (we calculated approximately as 0.1 mg due to the body weight changes during the treatment period of 30 days). A 250–275 g rat approximately consumes 25 g of chow/day; hence 4 mg of chromium

(0.1/25  $\times$  1000 g) was mixed with 1 kg of rat chow. After the treatment period of 30 days, rats were anesthetized; hearts were isolated and subjected to 30 min of ischemia followed by 2 h of reperfusion.

### 2.3. Isolated working heart preparation

Rats were given an intraperitoneal bolus of heparin (500 IU kg<sup>-1</sup>) and were anesthetized by the intraperitoneal administration of pentobarbital sodium (80 mg kg<sup>-1</sup>, Abbot, Baxter Health Care, Deep Field, IL). After ensuring a sufficient depth of anesthesia, a thoracotomy was performed; the hearts were rapidly excised and transferred into container having chilled Krebs Henseleit Bicarbonate perfusion Buffer (KHB, 118 mM NaCl, 4.7 mM KCl, 1.7 mM CaCl<sub>2</sub>, 25 mM NaHCO<sub>3</sub>, 1.2 mM KH<sub>2</sub>PO<sub>4</sub>, 1.2 mM MgSO<sub>4</sub>, 10 mM glucose). The aorta was cannulated, the hearts were subjected to retrograde perfusion on a Langendorff perfusion system at a hydrostatic pressure of 100 cm of H<sub>2</sub>O where the buffer was continuously oxygenated and maintained at a constant temperature of 37 °C [29,30]. The pulmonary vein was cannulated to another cannula to continue with the isolated working heart procedure. The Langendorff preparation was switched to the antegrade working mode, following a brief washout period, by switching the supply of the perfusate (maintained at a hydrostatic pressure of 17 cm of H<sub>2</sub>O) from the aorta to the left atrium. After the attainment of steady state, cardiac baseline functional parameters were recorded. The circuit was then switched back to the retrograde mode and the hearts were perfused for 5 min with KHB buffer, and were then subjected to 30 min of global ischemia followed by 2 h of reperfusion in antegrade working heart mode and the functional parameters were recorded at 30, 60, 90 and 120 min of reperfusion [29,30].

### 2.4. Cardiac function

Aortic pressure was measured using a pressure transducer (Micro-Med, Inc.) and the signal was amplified using a HPA-400 (Micro-Med, Inc, USA). The Heart Rate (HR), Left Ventricular Developed Pressure (LVDP), and (dp/dt<sub>max</sub>) were all derived from the continuously obtained pressure signal. Aortic flow (AF) was measured using a calibrated flow meter (Gilmont Instrument Inc., Barrington, IL, USA) and coronary flow (CF) was measured by timed collection of the coronary effluent dripping from the heart [29,30].

### 2.5. Measurement of infarct

At the end of reperfusion, the heart was perfused with a 1% (w/v) solution of triphenyl tetrazolium chloride in phosphate buffer through the aortic cannula for 1 min at 37 °C. To quantify the areas of interest in pixels, Scion image analysis software was used. The infarct size was quantified and was expressed in percentage [29,30].

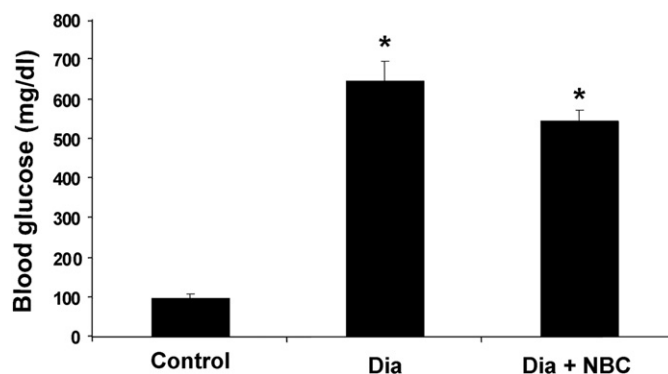
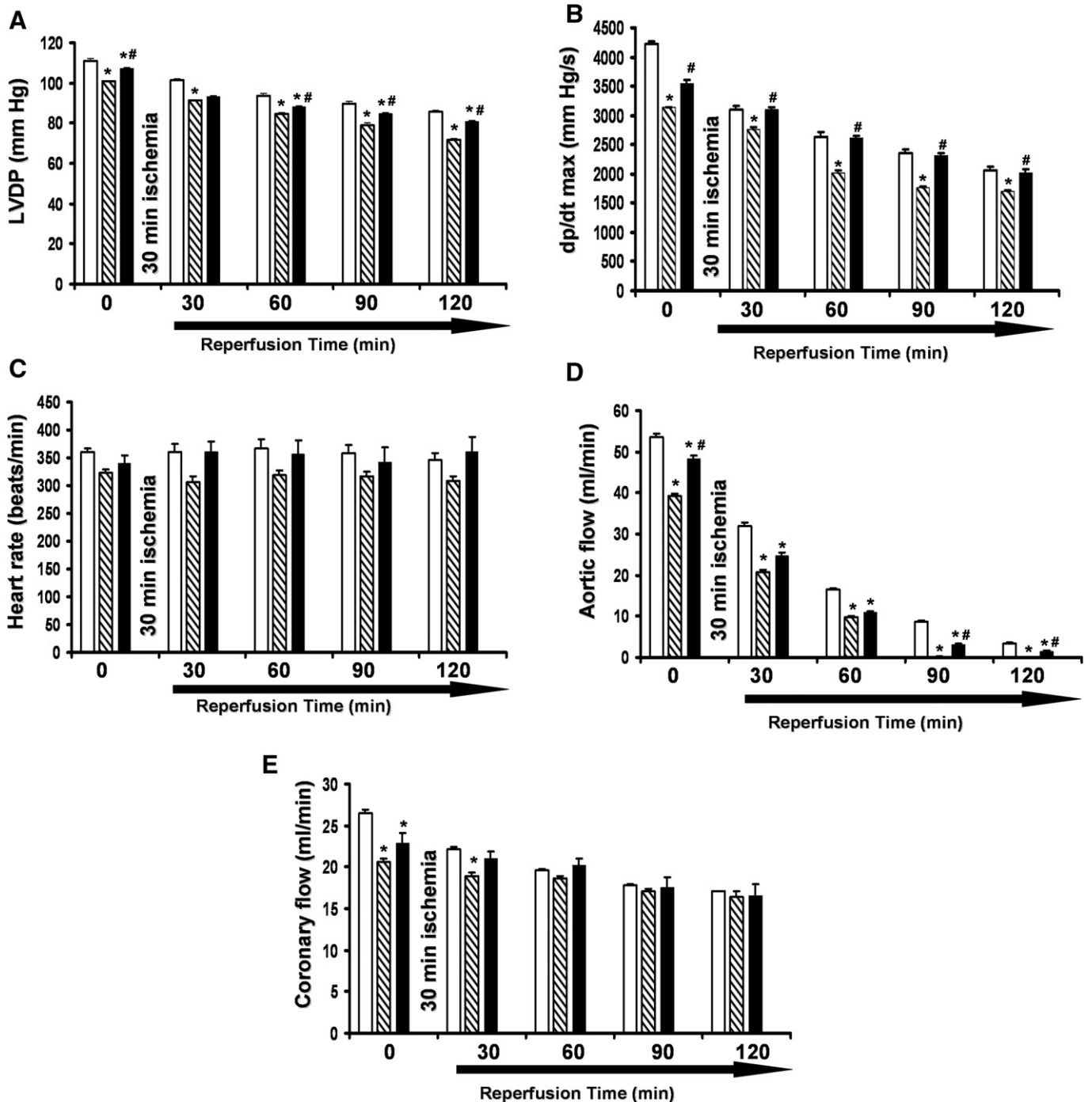


Fig. 1. Effect of NBC on blood glucose levels. \* $p<0.05$  compared with control.

## 2.6. Cardiomyocyte apoptosis

The formaldehyde-fixed left ventricle was embedded in paraffin and were cut into transverse sections (4  $\mu$ m thick) and deparaffinized with a graded series of histoclear and ethanol solutions. Immunohistochemical detection of apoptotic cells was carried out using TUNEL reaction using In Situ Cell Death Detection Kit, Fluorescein as per the kit protocol (Roche Diagnostics, Mannheim, Germany). In brief, the TUNEL reaction preferentially labels DNA strand breaks generated during apoptosis which can be identified by labeling free 3'-OH

termini with modified nucleotides in an enzymatic reaction catalysed by Terminal deoxynucleotidyl transferase (TdT). Fluorescein labels incorporated in nucleotide polymers are detected by fluorescence microscopy. The sections ( $n=5$ ) were washed thrice in PBS, blocked with 10% normal goat serum in 1% BSA in PBS and incubated with mouse monoclonal anti- $\alpha$ -sarcomeric actin (Sigma, St Louis, MO, USA) followed by staining with TRITC-conjugated rabbit anti-mouse IgG (1:200 dilution, Sigma, St Louis, MO, USA). After incubation, the sections were rinsed thrice in PBS and mounted with Vectashield mounting medium (Vector, Burlingame, CA). The sections were



**Fig. 2.** Effect of NBC on cardiac functional parameters at baseline (BL) and after 30 min of ischemia at 30, 60, 90 and 120 min of reperfusion. The results in (A) represent LVDP, (B) represents  $dp/dt_{max}$ , (C) represents heart rate, (D) represents aortic flow, (E) represents coronary flow. Results are shown in six animals per group. \* $p < 0.05$  compared with control, # $p < 0.05$  compared with Diabetic group. Where white bar represents Control, diagonal line bar represent diabetic group and black bar represents Dia+NBC group.

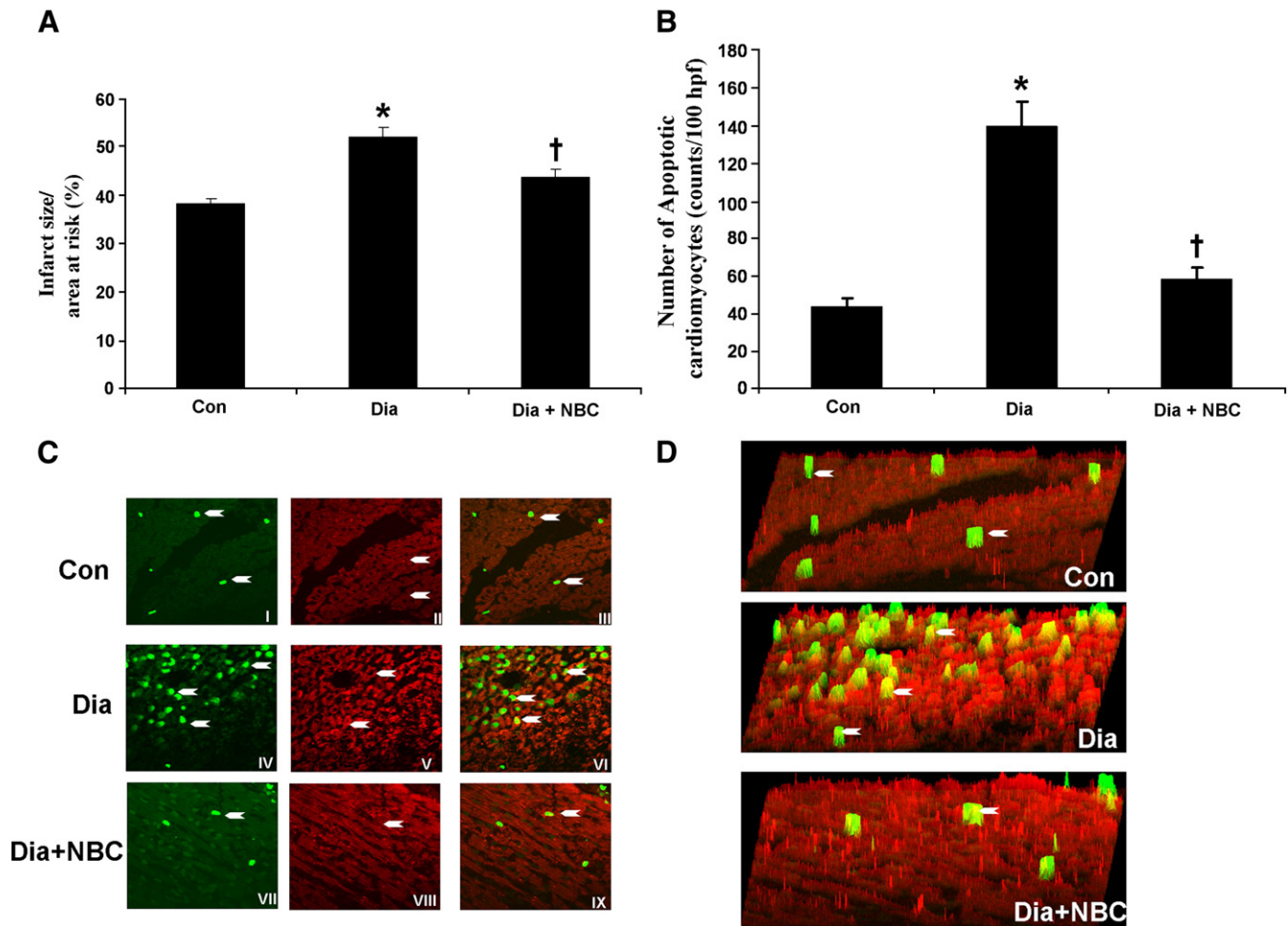


**Fig. 3.** (A) Graph represents the infarct size between the comparative groups. (B) Graph represents the number of apoptotic cardiomyocytes between the comparative groups. \* $p < 0.05$  compared with control and † $p < 0.05$  compared with diabetic group. (C) Figures represent apoptotic cells identified with anti  $\alpha$ -sarcomeric actin specific for cardiomyocytes. I–III represent the control group, IV–VI represent the diabetic group and VII–IX represent the Diabetic+NBC group. The white arrows represent the apoptotic cardiomyocytes stained by TUNEL assay. (D) The representative pictures for quantitative measurement of apoptotic cardiomyocytes using the Metamorph software.

observed and images were captured using a confocal laser Zeiss LSM 410 microscope. For the quantitative purpose, the number of TUNEL-positive cardiomyocytes was counted on 100 high power fields (HPF) [29].

### 2.7. Isolation of caveolin-rich (lipid raft) fractions

100 mg of tissue was homogenized in 2 ml of sucrose buffer (250 mM sucrose, 25 mM Tris (pH 7.4), 2 mM EDTA, 150 mM NaCl, 1% Triton X-100, and protease inhibitor cocktail) according to the modified protocol of Liu et al. [31] using a Polytron homogenizer as described by Koneru S et al. [10]. Sucrose gradients were prepared (5%, 30%, and 80%) in TNE (25 mM Tris HCl pH 7.5, 150 mM NaCl, 1 mM EGTA) buffer. The lysate was passed through a 23-gauge needle, and was then sonicated. Following sonication, 2 ml of 80% sucrose was added and mixed to make the sucrose concentration to 40% (1:1 dilution). On the top of this, 4 ml of 30% sucrose was layered, followed by 4 ml of 5% sucrose solution (total volume = 12 ml). The tubes containing sucrose gradient were centrifuged at 33,000 rpm for 17 h. Following centrifugation, the gradient was separated into 12 fractions of 1 ml each. The fractions 4–6 were considered as the lipid raft fractions and the fractions 8–12 were considered as the heavier fractions. Equal amount of tissue (100 mg) was used for all the groups, and the protein was estimated after isolation of the fractions. Equal amount of protein was loaded for all the groups to perform western blot analysis.

### 2.8. Isolation of cytosolic proteins

Left ventricular tissues from each group were homogenized and suspended (70 mg/ml) in sample buffer [10 mM HEPES, pH 7.3, sucrose 11.5%, EDTA 1 mM, EGTA 1 mM, diisopropylfluorophosphate (DFP), pepstatin A 0.7 mg/ml, leupeptin 10 mg/ml, aprotinin 2 mg/ml]. The homogenates were centrifuged at 3,000 rpm and the supernatant was collected and again centrifuged at 10,000 rpm for the cytosolic fraction. The total protein concentration was determined using BCA (bicinchoninic acid) protein assay kit (Pierce, Rockville, IL) [29].

### 2.9. Immunoprecipitation for Cav-1/eNOS and Cav-3/GLUT-4 association

To observe the association of Cav-1/eNOS and Cav-3/Glut-4 in the lipid raft fractions immunoprecipitation was performed in caveolin-rich fractions (fractions 4–6). Immunoprecipitation was performed with protein-A and protein-G Sepharose beads from Amersham Biosciences (Piscataway, NJ) using a polyclonal antibody against Cav-1 and Cav-3 monoclonal antibody from Santa Cruz Biotechnology (Santa Cruz, CA). The procedure was carried out according to the manufacturer's protocol. The caveolin-rich fractions (fractions 4–6) were immunoprecipitated with Cav-1 and Cav-3, which were reblotted with eNOS and Glut-4, respectively [10].



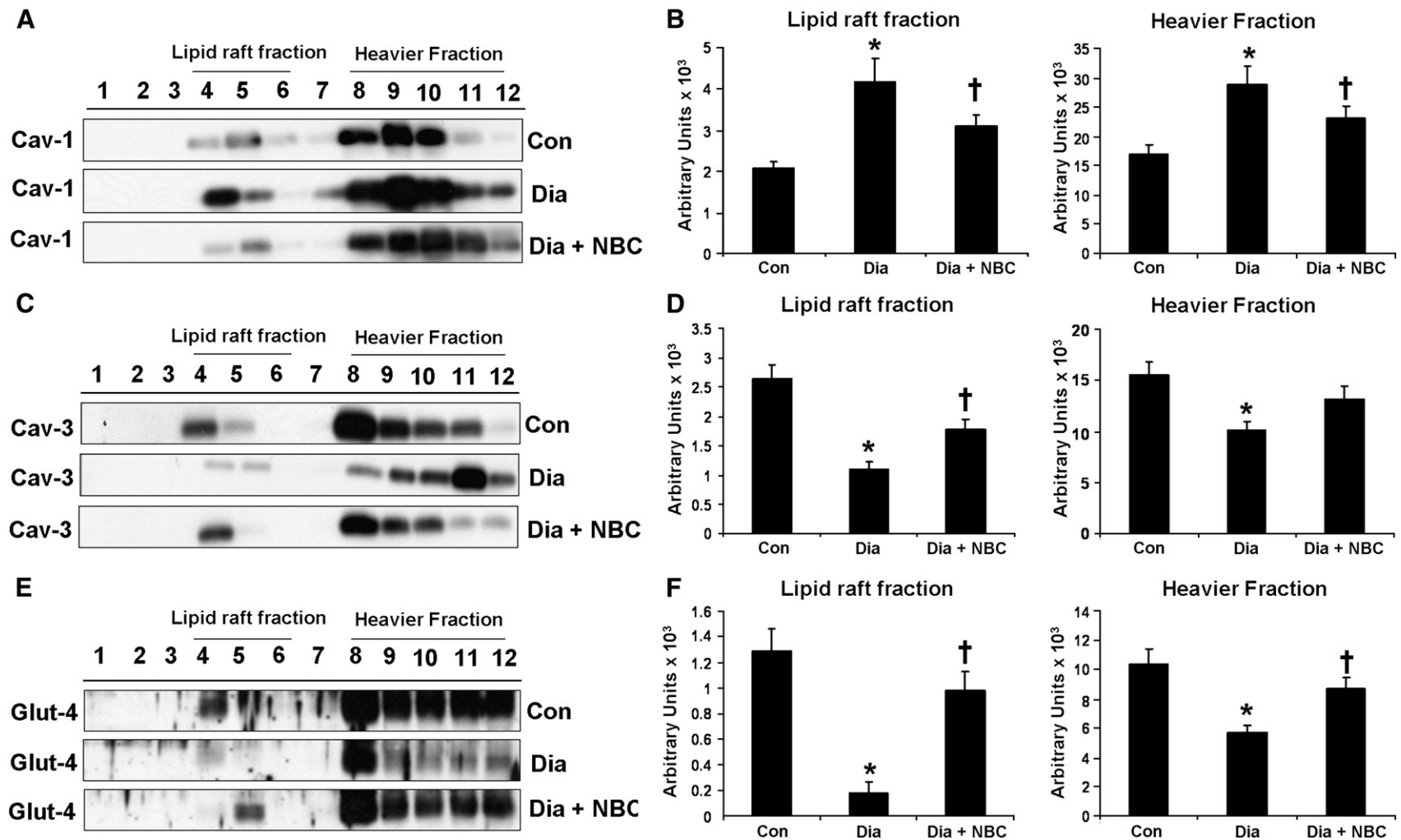


**Fig. 4.** (A) Represents the caveolin-1 protein expression in sucrose gradient fractions. (B) Represents the quantitative estimation of caveolin-1 both in the lipid raft fractions (4–6) fractions as well as heavier (8–12) fractions. (C) Represents the caveolin-3 protein expression in sucrose gradient fractions. (D) Represents the quantitative estimation of caveolin-3 both in the lipid raft fractions (4–6) fractions as well as heavier (8–12) fractions. (E) Represents the Glut-4 protein expression in sucrose gradient fractions. (F) Represents the quantitative estimation of Glut-4 both in the lipid raft fractions (4–6) fractions as well as heavier (8–12) fractions. \* $p < 0.05$  represents the significant difference between control and diabetic group. † $p < 0.05$  represents significant difference between diabetic and NBC treated diabetic group.

### 2.10. Western blot analysis for Cav-1, Cav-3, Glut-4, p-AMPK, AMPK, p-eNOS, eNOS, p-Akt and Akt

To quantify the expression of Cav-1, Cav-3, Glut-4 in lipid raft fractions p-eNOS, eNOS, p-Akt, Akt, p-AMPK and AMPK in the cytosolic fraction, standard SDS-PAGE Western blot analysis was performed with the use of polyacrylamide electrophoretic gels (7%, 10%, and 12%; acrylamide-to-bis ratios depending on the molecular weight of the proteins) as described previously [10,29]. The antibodies were purchased (Cell Signaling Technology, Danvers, MA; Abcam, Cambridge, MA; and Santa Cruz Biotechnology, Santa Cruz, CA) and were used at manufacturer-recommended dilutions.

### 2.11. Immunohistochemistry of Caveolin-1/eNOS and Caveolin-3/Glut-4

Paraffin embedded tissue sections of 4  $\mu$ m thick were used for immunohistochemical analysis. The sections were deparaffinized using histoclear solution, 100% ethanol, 90% ethanol, 80% ethanol and 70% ethanol followed by Phosphate Buffered Saline (PBS) wash. Each step was carried for 5 min. Slides were placed in boiling antigen retrieval buffer for 15 min and was then allowed to cool at room temperature for 20 min. Again, the slides were rinsed in PBS. The sections were rinsed with 0.5% BSA in PBS for 20 min. The slides were blocked in 10% normal donkey serum with 1% BSA in PBS for 2 h. For Glut-4 the sections were rinsed and blocked with 0.4% triton-X 100 along with BSA. After blocking the sections was incubated overnight with primary antibodies for Cav-1 (Santa Cruz Biotechnology) Cav-3, eNOS (BD Pharmingen, San Diego, CA) and Glut-4 (Chemicon International, Temecula, CA) diluted with 1% BSA in PBS overnight at room temperature. All primary antibodies were diluted at 1:100 ratios. After overnight incubation the sections were washed in PBS. The sections were rinsed with 0.5% BSA in PBS for 3 times for 5 min each. The sections were incubated with secondary antibodies Alexa flour 555 anti-rabbit (for Cav-1), anti-goat (for Glut-4) and Alexa flour 488 anti-mouse (for Cav-3 and eNOS) from Invitrogen, Eugene, Oregon, USA. The secondary antibodies were diluted with 1% BSA in PBS. The sections were incubated in secondary for 2 h. After incubation the sections were rinsed in PBS and mounted with citifluor mounting medium (Vector Laboratories Inc, Burlingame, CA 94010). The sections were observed and pictures were taken using Confocal 410 microscope [10].

### 2.12. Statistical analysis

Results are expressed as mean  $\pm$  standard deviation of the mean ( $\pm$ SD). ANOVA followed by Bonferroni's correction was carried out to determine any differences between the mean values of all groups. The results were considered significant if  $p < 0.05$ .

## 3. Results

### 3.1. Effect of NBC on the glucose level

Blood glucose levels were significantly increased in the diabetic rats when compared to non-diabetic rats. Treatment with NBC decreased the blood glucose level in Dia+NBC group as compared to Dia group (Fig. 1) however significant difference was not found between the groups.

### 3.2. Effect of NBC on cardiac functions

Significant reduction in the cardiac functional parameters such as LVDP (mm Hg),  $dp/dt_{max}$  (mm Hg/s), coronary flow (ml/min), and aortic flow (ml/min) except for the heart rate (beats/min) was observed in the diabetic group as compared to the control group at the baseline as well as during the 2 h of reperfusion.

The baseline abnormalities in heart function in STZ-diabetic myocardium may be due to the production of reactive oxygen species. However upon NBC treatment there was significant improvement of the cardiac functions at the baseline levels as well as during the 2 h of reperfusion. Aortic flow, maximum first derivative of developed pressure ( $dp/dt_{max}$ ) and left ventricular developed pressure of reperfusion were found to be significantly improved in NBC treated diabetic rats throughout the reperfusion time compared to untreated diabetic group. At the end of reperfusion time (after 120 min of reperfusion), the  $dp/dt_{max}$  (2020 vs 1691, mm Hg/s), aortic flow (1.5 ml vs 0 ml/min) and left ventricular developed pressure (80 vs 71 mm of Hg) were found to be significantly improved in the NBC treated diabetic group compared with the non-treated diabetic control (Fig. 2A–E).

### 3.3. Effect of NBC on infarct size and cardiomyocyte apoptosis

The infarct size and cardiomyocyte apoptosis was measured in all the groups after subjecting the hearts to 30 min of global ischemia and 2 h of reperfusion. Significant increase in the infarct size was observed in the diabetic group as compared to control (37% vs 51%). NBC treatment has significantly reduced the infarct size as compared to the diabetic group (51% vs 43%) (Fig. 3A). No significant difference was observed between the non-diabetic control and the NBC treated diabetic group. Similarly, significant increase in the cardiomyocyte apoptosis was observed in the diabetic group as compared to control. NBC treatment demonstrated significant reduction in the cardiomyocyte apoptosis as compared to the Diabetic group (58 vs 140 counts/100 HPF) (Fig. 3B). The representative pictures of cardiomyocyte apoptosis by TUNEL assay and the quantitative measurement of apoptotic cardiomyocytes using Metamorph software are shown in Fig. 3C and 3D.

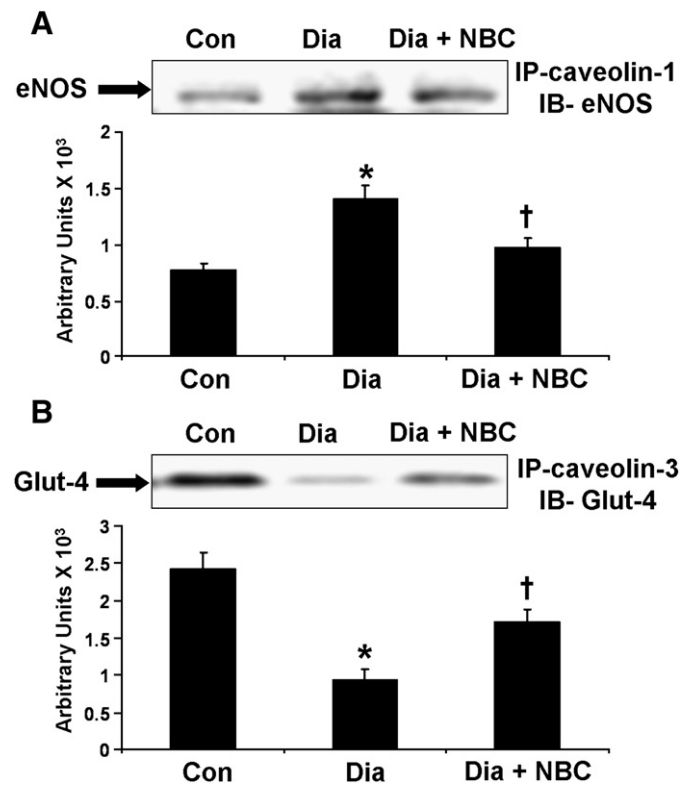


**Fig. 5.** (A) Immunoprecipitation with caveolin-1 and reblot with eNOS in control, Dia and Dia+NBC groups. (B) Immunoprecipitation with caveolin-3 and reblot with Glut-4 in control, Dia and Dia+NBC groups.  $n=6$  in each group. \* $p < 0.05$  represents the significant difference between control and diabetic group. † $p < 0.05$  represents significant difference between diabetic and NBC treated diabetic group.

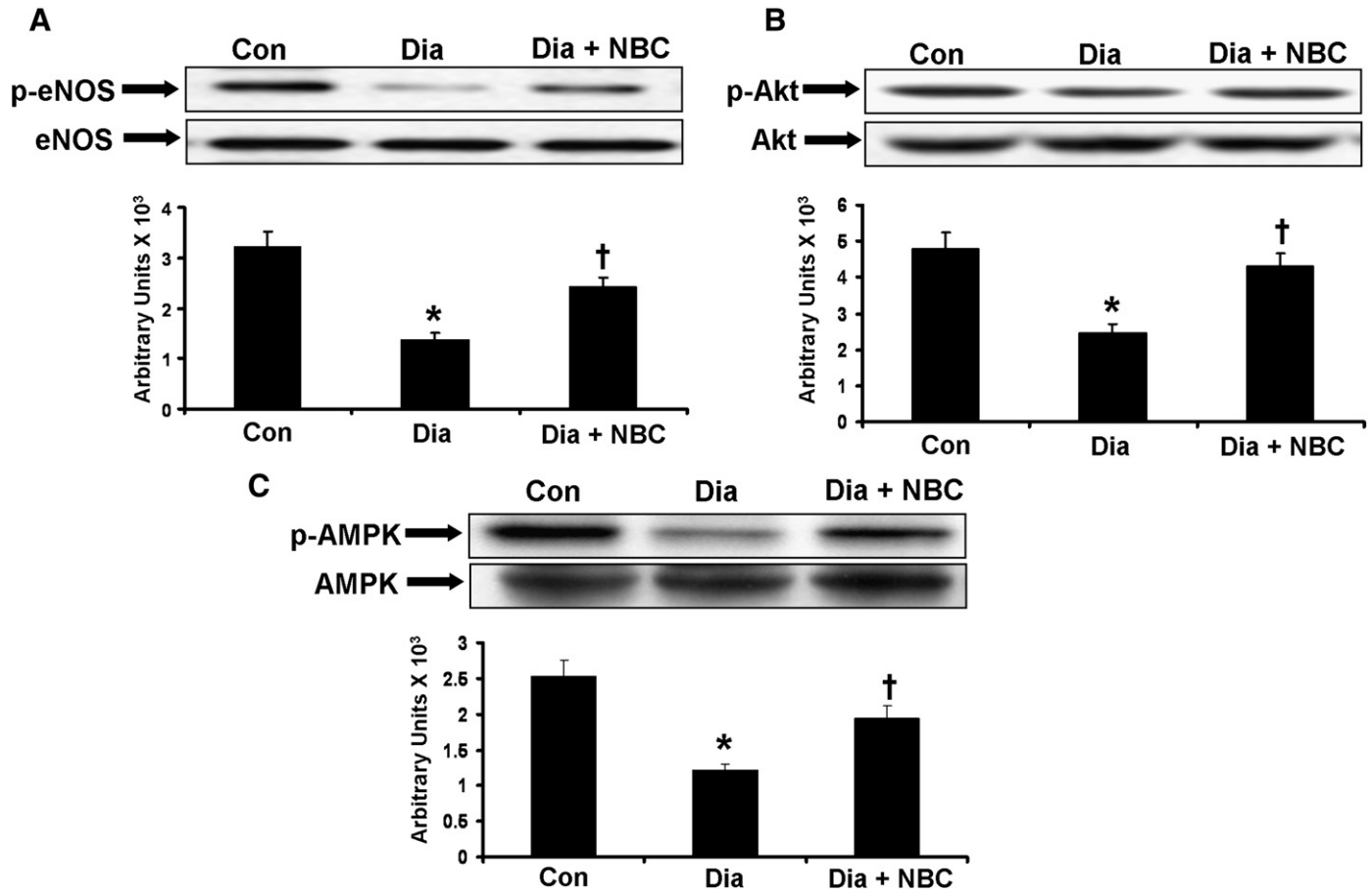


**Fig. 6.** (A) Represents the p-eNOS and eNOS protein. (B) Represents the p-Akt and Akt protein. (C) Represents the p-AMPK and AMPK expression in the cytosolic fraction. \* $p < 0.05$  represents the significant difference between control and diabetic group. † $p < 0.05$  represents significant difference between diabetic and NBC treated diabetic group.

#### 3.4. Effect of NBC on caveolin-1, caveolin-3 and Glut-4 expression in the sucrose gradient fractions

Significant increase in the caveolin-1 expression was observed in diabetic group as compared to control. NBC treatment has significantly reduced the level of caveolin-1 both in the lipid raft (fractions 4–6) and heavier (fractions 8–12) fractions when compared to diabetic group (Fig. 4A and B). Reverse pattern was observed in the caveolin-3 expression. Caveolin-3 expression was significantly reduced in the diabetic group as compared to control. NBC treatment has significantly increased the expression of caveolin-3 both in lipid raft (fractions 4–6) and heavier fractions (fractions 8–12) when compared to diabetic group (Fig. 4C and D). Upon NBC treatment increased expression of Glut-4 was observed in lipid raft and heavier fractions when compared to diabetic group. Increased Glut-4 in the lipid raft fraction in NBC group might be due to increased translocation of Glut-4 following NBC treatment (Fig. 4E and F). As expected, decreased expression of Glut-4 was observed both in lipid raft as well as in heavier fractions in the diabetic group compared to non-diabetic control. However, the ratio of Glut-4 translocation in comparison with lipid raft and heavier fractions between the groups was significantly lower in the diabetic group as compared to control and NBC treated groups. The control and treated group demonstrated 1:8 fold of Glut-4 translocation into the membrane but in the case of diabetic group only 1:30 fold of Glut-4 translocation to the membrane was observed.

#### 3.5. Effect of NBC on caveolin-1/eNOS and caveolin-3/Glut-4 association

Immunoprecipitation assay was performed to show the association of caveolin-1/eNOS and caveolin-3/Glut-4 in the caveolar rich

lipid raft (fractions 4–6) during diabetes and NBC treatment. Immunoprecipitation of Cav-1 and immunoblotting with eNOS clearly demonstrated that in diabetic group eNOS is significantly associated with Cav-1 as shown in Fig. 5A. During NBC treatment we have observed dissociation of cav-1 and eNOS which might have resulted in increased phosphorylation of eNOS in the cytosol. In a similar manner caveolin-3 was immunoprecipitated and reblot with Glut-4. Decreased association of Glut-4 and caveolin-3 was observed in diabetic group as compared to control group (Fig. 5B). NBC treatment documented increased association of Glut-4 and Cav-3 as compared to DM.

#### 3.6. Effect of NBC on phosphorylation of AMPK, Akt and eNOS in the cytosol

Phosphorylation of eNOS was found to be decreased in cytosol of diabetic group and NBC treatment has shown significant increase in the p-eNOS as compared to diabetic group (Fig. 6A). Decreased eNOS phosphorylation in diabetic group might be due to increased cav-1/eNOS interaction or association which possibly made eNOS unavailable for its activation. Similarly, phosphorylation of Akt was found to be decreased in cytosol of diabetic group and NBC treatment has shown significant increase in the p-Akt as compared to diabetic group (Fig. 6B). The phosphorylation of AMPK was also found to be reduced in diabetic group as compared to non-diabetic control. Upon NBC treatment phosphorylation of AMPK significantly increased as compared to the non-treated diabetic control (Fig. 6C). The non phosphorylated forms of these proteins were used as their corresponding loading controls.

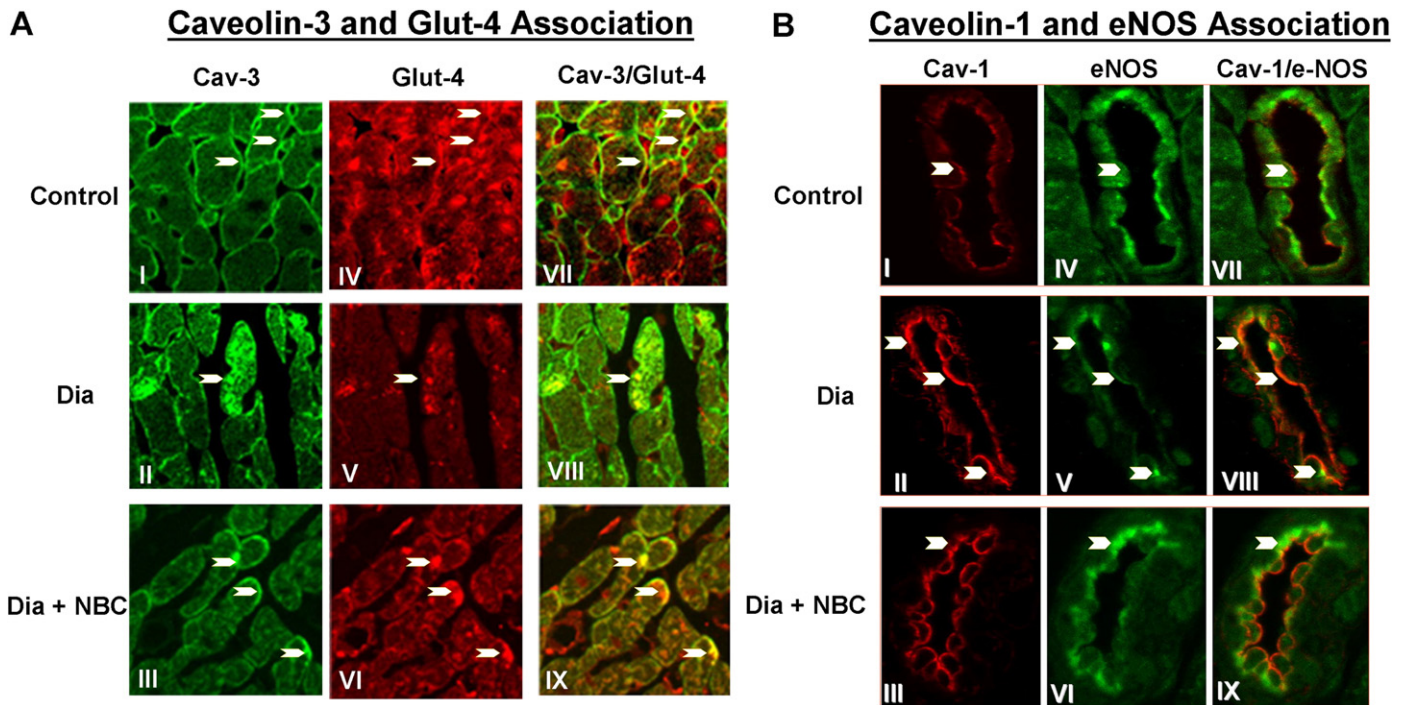


**Fig. 7.** (A) Represents the rat cardiac paraffin sections labeled with immunofluorescence and visualized using confocal microscopy (400 $\times$ ). I, II and III represent the green fluorescence labeled caveolin-3. IV, V and VI represent red fluorescence labeled Glut-4. VII, VIII and IX represent the merged picture which clearly shows the co-localization of caveolin-3 and Glut-4. White arrows denote the caveolin-3 and Glut-4 association. I, IV and VII represent control group, II, V and VIII represent Diabetic group and III, VI and IX represent Diabetic+NBC group. (B) Represents the rat cardiac paraffin sections labeled with immunofluorescence and visualized using confocal microscopy (400 $\times$ ). I, II and III represent the red fluorescence labeled caveolin-1. IV, V and VI green fluorescence labeled eNOS. VII, VIII and IX represent the merged picture which clearly shows the co-localization of caveolin-1 and eNOS. White arrows denote the caveolin-1 and eNOS association. I, IV and VII represent control group, II, V and VIII represent Diabetic group and III, VI and IX represent Diabetic+NBC group.

### 3.7. Immunohistochemical analysis of Cav-1/eNOS and Cav-3/Glut-4 association

Western blot analysis was also further confirmed by immunohistochemical analysis. The immunohistochemical analysis documented significant decrease in the expression of Cav-3 and increase in the Cav-1 in the membrane of diabetic group as compared to control [Fig. 7A (II) and B (II)]. As expected, on treatment with NBC converse results were obtained as compared to diabetic group [Fig. 7A (III) and B (III)]. Moreover, significant association of Cav-1/eNOS in the membrane was observed in the diabetic group as compared to control [Fig. 7B (VIII)]. On NBC treatment Cav-1/eNOS association was found to be decreased as compared to the diabetic group [Fig. 7B (IX)]. DM has shown decreased Glut-4 translocation to the membrane and association with caveolin-3 as compared to control [Fig. 7A (VIII)]. On NBC treatment increased Glut-4 translocation and association with caveolin-3 was observed as compared to diabetic group [Fig. 7A (IX)].

## 4. Discussion

In the present study we report the effect of Niacin-bound Chromium (NBC) in regulation of Glut-4 translocation in STZ-induced diabetic rats. The result of the present study clearly demonstrates NBC mediated Glut-4 expression and translocation might be mediated by modulating the Cav-1 and Cav-3 status in diabetic myocardium after IR injury. Dissociation of Cav-1/eNOS interaction, increased translocation of Glut-4 and its association with caveolin-3 with increased phosphorylation of AMPK, Akt and eNOS was observed upon NBC treatment. However, at present we don't know whether there is any alteration in glucose uptake or metabolism.

Our results suggest that NBC mediated Glut-4 translocation may be through the activation of the AMPK/Akt/eNOS signaling cascade, which is further regulated by the Cav-1 and Cav-3 status.

Significant reduction in the phosphorylation of AMPK was observed in diabetic group as compared to non-diabetic control. The key role of AMPK in the heart is the regulation of energy metabolism [32]. Large amounts of ATP are necessary to sustain contractile function and basal metabolism in a normal heart and this is primarily generated by mitochondrial oxidative metabolism, with a small amount derived from glycolysis [32]. Cardiac function is also dependent on the production of intracellular ATP derived from glucose metabolism [33]. NBC treatment increased the phosphorylation of AMPK as compared to the non-treated diabetic control. This significant increase in the levels of p-AMPK correlate with the improvement of the cardiac functions during reperfusion in the NBC treated group as compared to the non-treated diabetic group. AMP-activated protein kinase functions as a metabolic master switch which senses and regulates the cellular energy status in various cells [24]. AMPK has also been reported to induce Glut-4 upregulation and translocation to the membrane after ischemic preconditioning [11]. Moreover, enhanced Glut-4 translocation and increased glucose uptake by 5-aminoimidazole-4-carboxy-amide-1- $\beta$ -D-ribofuransoside (AICAR) was found to be mediated by activation of AMPK [26]. We have observed decreased Glut-4 expression in the membrane fractions of the diabetic group as compared to the normal control. However, NBC treatment increased the expression of Glut-4 in the membrane fractions as compared to the non-treated diabetic control animals. This observation agrees with previous reports that AMPK activates the expression and translocation of Glut-4 [27]. Glut-4 is the major insulin-responsive glucose transporter that clears glucose from the blood. In the absence of insulin, Glut-4 is sequestered into specialized storage vesicles that remain within the cell [9]. AMPK is also known to phosphorylate eNOS at Ser 1177 rendering it active [23]. We have documented decreased expression of p-eNOS in the diabetic group as compared to the normal control. Upon NBC treatment the expression of p-eNOS significantly increased in the treated group



as compared to the non-treated diabetic control. eNOS is the source of NO and is important in regulation of blood pressure, vascular remodeling, vasodilation, angiogenesis and wound healing [24]. The vasodilatory function of eNOS might explain the improved aortic flow in the NBC treated group as compared to the non-treated diabetic control. eNOS is also known to be regulated by Akt/PKB [34].

Akt/PKB is a critical central signaling node, downstream of many growth factors. Akt substrates contribute to the diverse cellular roles including cell survival, growth, proliferation, angiogenesis, metabolism, and migration [35]. It has been reported that Akt enhances the survival of cells by blocking the function of proapoptotic proteins and processes [36]. Phosphorylation of Akt has also been known to play a very important role in facilitating growth factor-mediated cell survival and in blocking apoptotic cell death [37]. Reports have also shown that phosphorylation and activation of Akt play an essential role in Glut-4 translocation as well by being involved in docking and/or fusion of Glut-4 vesicles with the cell surface [38,39]. In our present study we have also observed significantly increased p-Akt in the NBC treated group as compared to the non-treated diabetic control. However, p-Akt was significantly decreased in the diabetic group as compared to the non-diabetic control. This activation of p-Akt explains the activation of the survival pathway in the NBC treated group and hence the significant decrease in the number apoptotic cardiomyocytes and improved functions as compared to the diabetic control after ischemia reperfusion.

Our previous results have shown that eNOS activity is also known to be regulated by differential regulation of the Cav-1 [10]. Endothelial nitric oxide synthase (eNOS) is one of the many proteins tethered to Cav-1. Bucci et al. have reported the regulation of eNOS activity by Cav-1 [40,41]. The expression of Cav-1 in the endothelial cells seems to be directly linked to the inhibition of NO synthesis [42]. In the present study our results demonstrate significant increase in the expression of Cav-1 in the diabetic group while NBC treatment significantly reduced the expression of Cav-1 as compared to the non-treated diabetic control. In addition, McCarty has demonstrated that nitric oxide deficiency, the crucial factor for pathogenesis during diabetes can be prevented by antioxidants, essential fatty acids and chromium supplementation [43]. Furthermore, immunohistochemical and immuno-precipitation analysis for Cav-1/eNOS association has also shown significant increase in the Cav-1/eNOS association in the diabetic group in the membrane as compared to the non-diabetic control. As expected, NBC treatment disrupted the Cav-1/eNOS association releasing eNOS, thus increasing its availability as a target substrate for phosphorylation for both activated AMPK and Akt. This explains our observation of increased p-eNOS in the NBC treated group and how its activation is inversely proportional to the expression of Cav-1.

On the other hand, Cav-3 expression was significantly decreased in the diabetic group in the caveolar lipid raft fractions when compared to the non-diabetic control. Caveolin 3 knockout mice (Cav3<sup>-/-</sup>) have been reported to show increased adiposity and insulin resistance [19]. NBC treatment significantly increased the expression of Cav-3 in lipid raft fractions in the treatment group as compared to the non-treated diabetic control. Immunohistochemical analysis has shown increased association of Glut-4 and Cav-3 in the NBC treated group as compared to the non-treated diabetic control which was further validated by immuno-precipitation. However, this association was significantly reduced in the diabetic group as compared to the non-diabetic control. Earlier reports have shown that Glut-4 translocates to the caveolin-enriched membrane domains after insulin stimulation in adipocytes [44,45]. Karlsson et al. have demonstrated morphologically and biochemically that, in the plasma membrane of adipocytes Glut-4 is localized in caveolae resulting in glucose uptake [46]. Moreover, disruption of caveolae was shown to make adipose cells insulin resistant [47]. These reports suggest that caveolin signaling plays an important role in Glut-4 translocation and

glucose uptake. Increased expression of Cav-3 along with Glut-4 and their association in NBC treated diabetic myocardium supports the notion that Glut-4 translocation occurs to the caveolae in the membrane and Cav-3 tethers Glut-4 to the cell surface lipid raft domains when stimulated.

To summarize, NBC mediated Glut-4 translocation may be mediated by 1) disruption of the Cav-1/eNOS interaction resulting in increased phosphorylation of eNOS 2) increase in the activation of AMPK and Akt 3) increase in the association of Glut-4 and Cav-3 in the membrane. The reduction in infarct size and cardiomyocyte apoptosis in NBC treated diabetic myocardium might be due to the activation of Akt and eNOS. However, further investigations are necessary to confirm the protective role of NBC in caveolin signaling during ischemia reperfusion in diabetic animals.

## Acknowledgement

This study was supported by InterHealth Research Center (Benicia, CA).

## References

- [1] R.A. Anderson, Chromium, glucose intolerance and diabetes, *J. Am. Coll. Nutr.* 17 (1998) 548–555.
- [2] R.A. Anderson, M.M. Polansky, N.A. Bryden, S.J. Bhatthena, J.J. Canary, Effects of supplemental chromium on patients with symptoms of reactive hypoglycemia, *Metabolism* 36 (1987) 351–355.
- [3] J.B. Vincent, Mechanisms of chromium action: low-molecular-weight chromium-binding substance, *J. Am. Coll. Nutr.* 18 (1999) 6–12.
- [4] C.M. Davis, J.B. Vincent, Chromium oligopeptide activates insulin receptor tyrosine kinase activity, *Biochemistry* 36 (1997) 4382–4385.
- [5] G. Chen, P. Liu, G.R. Pattar, L. Tackett, P. Bhonagiri, A.B. Strawbridge, J.S. Elmendorf, Chromium activates glucose transporter 4 trafficking and enhances insulin-stimulated glucose transport in 3T3-L1 adipocytes via a cholesterol-dependent mechanism, *Mol. Endocrinol.* 20 (2006) 857–870.
- [6] D. Pei, C.H. Hsieh, Y.J. Hung, J.C. Li, C.H. Lee, S.W. Kuo, The influence of chromium chloride-containing milk to glycemic control of patients with type 2 diabetes mellitus: a randomized, double-blind, placebo-controlled trial, *Metabolism* 55 (2006) 923–927.
- [7] A. Shinde Urmila, G. Sharma, J. Xu Yan, S. Dhalla Naranjan, K. Goyal Ramesh, Anti-diabetic activity and mechanism of action of chromium chloride, *Exp. Clin. Endocrinol. Diabetes* 112 (2004) 248–252.
- [8] N.A. Trueblood, R. Ramasamy, L.F. Wang, S. Schaefer, Niacin protects the isolated heart from ischemia-reperfusion injury, *Am. J. Physiol. Heart Circ. Physiol.* 279 (2000) H764–H771.
- [9] R.T. Watson, J.E. Pessin, Intracellular organization of insulin signaling and GLUT4 translocation, *Recent Prog. Horm. Res.* 56 (2001) 175–193.
- [10] S. Koneru, S.V. Penumathsa, M. Thirunavukkarasu, S.M. Samuel, L. Zhan, Z. Han, G. Maulik, D.K. Das, N. Maulik, Redox regulation of ischemic preconditioning is mediated by the differential activation of caveolins and their association with eNOS and GLUT-4, *Am. J. Physiol. Heart Circ. Physiol.* 292 (2007) H2060–H2072.
- [11] Y. Nishino, T. Miura, T. Miki, J. Sakamoto, Y. Nakamura, Y. Ikeda, H. Kobayashi, K. Shimamoto, Ischemic preconditioning activates AMPK in a PKC-dependent manner and induces GLUT4 up-regulation in the late phase of cardioprotection, *Cardiovasc. Res.* 61 (2004) 610–619.
- [12] D. Sun, N. Nguyen, T.R. DeGrado, M. Schwaiger, F.C. Brosius 3rd, Ischemia induces translocation of the insulin-responsive glucose transporter GLUT4 to the plasma membrane of cardiac myocytes, *Circulation* 89 (1994) 793–798.
- [13] R.G. Anderson, The caveolae membrane system, *Annu. Rev. Biochem.* 67 (1998) 199–225.
- [14] R. Hnasko, M.P. Lisanti, The biology of caveolae: lessons from caveolin knockout mice and implications for human disease, *Mol. Interv.* 3 (2003) 445–464.
- [15] H.H. Patel, Y.M. Tsutsumi, B.P. Head, I.R. Niesman, M. Jennings, Y. Horikawa, D. Huang, A.L. Moreno, P.M. Patel, P.A. Insel, D.M. Roth, Mechanisms of cardiac protection from ischemia/reperfusion injury: a role for caveolae and caveolin-1, *FASEB J.* 21 (2007) 1565–1574.
- [16] E.J. Smart, G.A. Graf, M.A. McNiven, W.C. Sessa, J.A. Engelman, P.E. Scherer, T. Okamoto, M.P. Lisanti, Caveolins, liquid-ordered domains, and signal transduction, *Mol. Cell Biol.* 19 (1999) 7289–7304.
- [17] I. Fleming, R. Busse, Signal transduction of eNOS activation, *Cardiovasc. Res.* 43 (1999) 532–541.
- [18] H. Park, Y.M. Go, R. Darji, J.W. Choi, M.P. Lisanti, M.C. Maland, H. Jo, Caveolin-1 regulates shear stress-dependent activation of extracellular signal-regulated kinase, *Am. J. Physiol. Heart Circ. Physiol.* 278 (2000) H1285–H1293.
- [19] F. Capozza, T.P. Combs, A.W. Cohen, Y.R. Cho, S.Y. Park, W. Schubert, T.M. Williams, D.L. Brasaemle, L.A. Jelicks, P.E. Scherer, J.K. Kim, M.P. Lisanti, Caveolin-3 knockout mice show increased adiposity and whole body insulin resistance, with ligand-induced insulin receptor instability in skeletal muscle, *Am. J. Physiol. Cell Physiol.* 288 (2005) C1317–C1331.

- [20] M. Bucci, F. Roviezzo, V. Brancaleone, M.I. Lin, A. Di Lorenzo, C. Cicala, A. Pinto, W.C. Sessa, S. Farneti, S. Fiorucci, G. Cirino, Diabetic mouse angiopathy is linked to progressive sympathetic receptor deletion coupled to an enhanced caveolin-1 expression, *Arterioscler. Thromb. Vasc. Biol.* 24 (2004) 721–726.
- [21] S. Dimmeler, I. Fleming, B. Fisslthaler, C. Hermann, R. Busse, A.M. Zeiher, Activation of nitric oxide synthase in endothelial cells by Akt-dependent phosphorylation, *Nature* 399 (1999) 601–605.
- [22] Y.C. Boo, G. Sorescu, N. Boyd, I. Shiojima, K. Walsh, J. Du, H. Jo, Shear stress stimulates phosphorylation of endothelial nitric-oxide synthase at Ser1179 by Akt-independent mechanisms: role of protein kinase A, *J. Biol. Chem.* 277 (2002) 3388–3396.
- [23] Z.P. Chen, K.I. Mitchelhill, B.J. Michell, D. Stapleton, I. Rodriguez-Crespo, L.A. Witters, D.A. Power, P.R. Ortiz de Montellano, B.E. Kemp, AMP-activated protein kinase phosphorylation of endothelial NO synthase, *FEBS Lett.* 443 (1999) 285–289.
- [24] Y. Zhang, T.S. Lee, E.M. Kolb, K. Sun, X. Lu, F.M. Sladek, G.S. Kassab, T. Garland Jr., J.Y. Shyy, AMP-activated protein kinase is involved in endothelial NO synthase activation in response to shear stress, *Arterioscler. Thromb. Vasc. Biol.* 26 (2006) 1281–1287.
- [25] L.H. Young, J. Li, S.J. Baron, R.R. Russell, AMP-activated protein kinase: a key stress signaling pathway in the heart, *Trends Cardiovasc. Med.* 15 (2005) 110–118.
- [26] R.R. Russell 3rd, R. Bergeron, G.I. Shulman, L.H. Young, Translocation of myocardial GLUT-4 and increased glucose uptake through activation of AMPK by AICAR, *Am. J. Physiol.* 277 (1999) H643–H649.
- [27] J. Li, X. Hu, P. Selvakumar, R.R. Russell 3rd, S.W. Cushman, G.D. Holman, L.H. Young, Role of the nitric oxide pathway in AMPK-mediated glucose uptake and GLUT4 translocation in heart muscle, *Am. J. Physiol. Endocrinol. Metab.* 287 (2004) E834–E841.
- [28] H.G. Preuss, S. Montamarry, B. Echard, R. Scheckenbach, D. Bagchi, Long-term effects of chromium, grape seed extract, and zinc on various metabolic parameters of rats, *Mol. Cell Biochem.* 223 (2001) 95–102.
- [29] M. Thirunavukkarasu, S.V. Penumathsa, B. Juhasz, L. Zhan, G. Cordis, E. Altaf, M. Bagchi, D. Bagchi, N. Maulik, Niacin-bound chromium enhances myocardial protection from ischemia-reperfusion injury, *Am. J. Physiol. Heart Circ. Physiol.* 291 (2006) H820–H826.
- [30] M. Thirunavukkarasu, S.V. Penumathsa, S. Koneru, B. Juhasz, L. Zhan, H. Otani, D. Bagchi, D.K. Das, N. Maulik, Resveratrol alleviates cardiac dysfunction in streptozotocin-induced diabetes: role of nitric oxide, thioredoxin, and heme oxygenase, *Free Radic. Biol. Med.* 43 (2007) 720–729.
- [31] Y. Liu, L. Casey, L.J. Pike, Compartmentalization of phosphatidylinositol 4,5-bisphosphate in low-density membrane domains in the absence of caveolin, *Biochem. Biophys. Res. Commun.* 245 (1998) 684–690.
- [32] J.R.B. Dyck, G.D. Lopaschuk, AMPK alterations in cardiac physiology and pathology: enemy or ally? *J. Physiol.* 574 (2006) 95–112.
- [33] C. Depre, J.L. Vanoverschelde, H. Taegtmeyer, Glucose for the heart, *Circulation* 99 (1999) 578–588.
- [34] D. Fulton, J.P. Gratton, T.J. McCabe, J. Fontana, Y. Fujio, K. Walsh, T.F. Franke, A. Papapetropoulos, W.C. Sessa, Regulation of endothelium-derived nitric oxide production by the protein kinase Akt, *Nature* 399 (1999) 597–601.
- [35] B.D. Manning, L.C. Cantley, AKT/PKB signaling: navigating downstream, *Cell* 129 (2007) 1261–1274.
- [36] J. Downward, PI 3-kinase, Akt and cell survival, *Semin. Cell Dev. Biol.* 15 (2004) 177–182.
- [37] S.R. Datta, A. Brunet, M.E. Greenberg, Cellular survival: a play in three Akts, *Genes Dev.* 13 (1999) 2905–2927.
- [38] P.-H. Ducluzeau, L.M. Fletcher, G.I. Welsh, J.M. Tavaré, Functional consequence of targeting protein kinase B/Akt to GLUT4 vesicles, *J. Cell Sci.* 115 (2002) 2857–2866.
- [39] M.M. Hill, S.F. Clark, D.F. Tucker, M.J. Birnbaum, D.E. James, S.L. Macaulay, A role for protein kinase B $\beta$ /Akt2 in insulin-stimulated GLUT4 translocation in adipocytes, *Mol. Cell Biol.* 19 (1999) 7771–7781.
- [40] M. Bucci, J.P. Gratton, R.D. Rudic, L. Acevedo, F. Roviezzo, G. Cirino, W.C. Sessa, In vivo delivery of the caveolin-1 scaffolding domain inhibits nitric oxide synthesis and reduces inflammation, *Nat. Med.* 6 (2000) 1362–1367.
- [41] S. Li, J. Couet, M.P. Lisanti, Src tyrosine kinases, Galpha subunits, and H-Ras share a common membrane-anchored scaffolding protein, caveolin. Caveolin binding negatively regulates the auto-activation of Src tyrosine kinases, *J. Biol. Chem.* 271 (1996) 29182–29190.
- [42] D. Fulton, J.-P. Gratton, W.C. Sessa, Post-translational control of endothelial nitric oxide synthase: why isn't calcium/calmodulin enough? *J. Pharmacol. Exp. Ther.* 299 (2001) 818–824.
- [43] M.F. McCarty, Nitric oxide deficiency, leukocyte activation, and resultant ischemia are crucial to the pathogenesis of diabetic retinopathy/neuropathy—preventive potential of antioxidants, essential fatty acids, chromium, ginkgolides, and pentoxifylline, *Med. Hypotheses* 50 (1998) 435–449.
- [44] J. Gustavsson, S. Parpal, P. Stralfors, Insulin-stimulated glucose uptake involves the transition of glucose transporters to a caveolae-rich fraction within the plasma membrane: implications for type II diabetes, *Mol. Med.* 2 (1996) 367–372.
- [45] P.E. Scherer, M.P. Lisanti, G. Baldini, M. Sargiacomo, C.C. Mastick, H.F. Lodish, Induction of caveolin during adipogenesis and association of GLUT4 with caveolin-rich vesicles, *J. Cell Biol.* 127 (1994) 1233–1243.
- [46] M. Karlsson, H. Thorn, S. Parpal, P. Stralfors, J. Gustavsson, Insulin induces translocation of glucose transporter GLUT4 to plasma membrane caveolae in adipocytes, *FASEB J.* 16 (2002) 249–251.
- [47] S. Parpal, M. Karlsson, H. Thorn, P. Stralfors, Cholesterol depletion disrupts caveolae and insulin receptor signaling for metabolic control via insulin receptor substrate-1, but not for mitogen-activated protein kinase control, *J. Biol. Chem.* 276 (2001) 9670–9678.